Transactions, **SMiRT-26**
Berlin/Potsdam, Germany, July 10-15, 2022
Division II - Fracture Mechanics and Structural Integrity

CONSIDERATION OF WELDING RESIDUAL STRESSES WITHIN THE FRACTURE MECHANICS ASSESSMENT OF NUCLEAR COMPONENTS – PART 2: FINITE ELEMENT MODELLING

Stéphane Chapuliot[1*], Anna Dahl[1], Stéphane Marie[2], Olivier Ancelet[2]

[1] EDF Expert, EDF/R&D, Materials & Mechanics of Components Department, France
[2] FRAMATOME Experts, FRAMATOME
*Corresponding author: stephane.chapuliot@edf.fr

INTRODUCTION - CONTEXT

Welding Residual Stresses (WRS) are a consequence of inhomogeneous thermal fields during the welding process. Self-equilibrated, they are of secondary nature and thus cannot contribute to the plastic collapse. However, for a low ductility material, they can contribute to the fracture process since they contribute to the stress field at the crack tip.

If this potential effect of WRS is well known, particularly in brittle fracture, it is also well known that, for high ductility material, the WRS are removed by the overall plastic flow in the ligament and thus become inoperant. Between those two extreme situations, the inherent difficulties regarding the consideration of WRS within Fracture Mechanics Assessment (FMA) is that the domain where they become non-significant is not clearly established. This is particularly true for the brittle to ductile transition of high ductility ferritic steels where a competition between brittle and ductile fracture is observed for the highest temperature of the ductile to brittle transition.

Behind this unclear definition of the influence domain of WRS, the fracture models conventionally used in FMA are too simple to capture correctly the real impact of WRS. Those are based on global approach parameters such as J or K_J which appear to be over-conservative when applied to real structures. The local approach criteria, much more complex to use, are better candidates for modelling fracture process with WRS, but they are limited to expertise applications and not generalisable to industrial applications.

The development of a limit defining the conditions when the WRS will impact the FMA is of strong interest since, with such limit, useless and non-physical modelling could be avoided. For that reason, EDF and FRAMATOME have initiated a cooperative R&D project for defining exclusion criteria for the WRS consideration within FMA. This project is focussed on testing and modelling, as well as literature survey and pre-codification.

The present paper deals the part 2 devoted Finite Element Modelling (FEM) while part 1 presents the analysis of the existing testing and modelling results in open literature. Those modelling are focused on industrial configurations and investigate, through the application of global and local approach criteria, the limits above which the WRS can be neglected within the FMA. Two configurations were chosen for that purpose:

- A large low alloy steel vessel submitted to a cold thermal shock.
- A Carbone-Manganese (C-Mn) pipe submitted to global bending.

For those two configurations, parametric numerical analyses are performed. It covers the WRS level, loading level, temperature and defect size. Both global and local approach criteria are applied, allowing to

illustrate the over-conservatism of the conventional global approach (K_{IC}) criterion in the highest temperatures of the brittle to ductile temperature range.
Based on those results, some criteria defining when WRS can be neglected in the FMA are initiated as well as perspectives for the continuation of this numerical work.

MATERIAL MODEL DESCRIPTION

Results from the Bibliography survey

The part 1 of this work dedicated to a literature survey [1] provided us a reliable experimental support for evaluating the capability of global and local approach criteria for quantifying the real impact of Residual Stresses (RS) on the fracture risk. This support is the test series performed by Hurlston *et al.* [2] on Three Point Bending (3PB) specimen where a lateral punching is imposed far from the crack tip for introducing reliable and reproducible RS fields. The data provided by the authors in [2] allowed us to perform a detailed FE analysis which allowed us to reach the following conclusions:

- The tests were performed relatively low in the brittle to ductile temperature range. For that condition, the global approach gives a correct estimate of the effect of RS on the risk of rupture. As an average value, the overestimation obtained here is estimated around 10% on the SIF for deep crack condition. For shallow crack conditions, the global approach remains pertinent since the RS increase the constraint at the crack tip. Without RS, the global approach does not capture the well-known shallow crack effect.
- At the opposite, the local approach criterion captures the shallow effect and, regarding the impact of RS, provides a correct estimation of the impact of the RS on the fracture probability.

Based on those results, the purpose of the following numerical analyses is to compare global approach and local approach predictions in industrial configurations. It is assumed here that the local approach provides the most reliable solution.

Local approach fracture model

General description:

For the present detailed analysis, we rely on the BEREMIN model [3] which is a local approach model dedicated to the brittle fracture of ferritic steels. In this model, the possible brittle failure is activated by plastic strain and then driven by the largest principal stress. For ferritic steels, brittle fracture is initiated at inclusions or grain boundaries depending on the size of those inclusions, the size or the crystallographic orientation of the grains. The brittle fracture of steels is therefore generally very dispersed.

To represent this fracture, the BEREMIN model is based on the weakest link assumption, that is to say that the initiation of one link leads to the complete rupture of the system. The representation is probabilistic, with a fracture probability of the link i defined according to the Weibull statistic, namely:

$$pr_i = \left(\frac{\sigma_I}{\sigma_u}\right)^m$$

σ_I is here the maximum principal stress, m and σ_u the parameters of the model. In the presence of a stress gradient, as is the case at the tip at a crack, a so-called Weibull stress (σ_W) is defined corresponding to the integration of the principal stress on the volume where the plasticity is active (noted V_p) at the tip of the crack:

$$\sigma_W = \left[\int_{V_p} \frac{\sigma_1^m}{V_0}\right]^{\frac{1}{m}}$$

V_0 is here a characteristic volume often associated with the average grain size. The application of the weakest link assumption (integration of the probabilities pr_i) then gives us:

$$Pr = 1 - exp\left[-\left(\frac{\sigma_W}{\sigma_u}\right)^m\right]$$

Such a model has 3 parameters, namely m, σ_u and V_0. But in practice σ_u and V_0 being linked together, the model is said to have 2 parameters.

The model is said to have 3 parameters when a threshold stress is introduced, this threshold stress (denoted σ_{th}) corresponding to the level of principal stress below which the risk of cleavage no longer exists. Two forms are possible to integrate this threshold stress into the Weibull stress:

$$\sigma_W = \left[\int_{V_p} \frac{(\sigma_I - \sigma_{th})^m}{V_0}\right]^{\frac{1}{m}}, \qquad ou : \sigma_W = \left[\int_{V_p} \frac{\sigma_1^m - \sigma_{th}^m}{V_0}\right]^{\frac{1}{m}}$$

In the present work, we prefer the first form of the Weibull stress, simpler to implement numerically. Other variants of the criterion integrate corrections associated to the plastic strain. We do not integrate this type of correction in the present work since it requires calibration on test campaigns integrating several different specimen geometries.

Data for the Low alloy steel: the FISTER material [4]:

For the definition of the fracture criterion, we rely on the two parameters BEREMIN model. FISTER database provides many fracture tests on CT25 specimens for the low alloy 16MND5 steel over the entire brittle to ductile transition. Based on these tests, it was possible to define a failure model depending on the temperature which reproduces well the behaviour of the material over the entire temperature range considered.

The model was calibrated through 3D FEM of CT specimen (50µm² square elements, $V_0 = 50\mu m^3$) providing the following σ_u stress:

$$Pr = 1 - exp\left[-\left(\frac{\sigma_W}{\sigma_u(\sigma_y)}\right)^m\right], \qquad \text{with: } \sigma_u(\sigma_y) = max\{3270; 5320 - 3.436.\sigma_y; 15250 - 24.44.\sigma_y\},$$

It can be noted that the material data σ_u is expressed here as a function of the yield stress σ_y to represent well the fracture resistance increasing with temperature. The modulus m is defined as a constant (m = 16.5). The Weibull stress σ_W is calculated here without threshold stress.

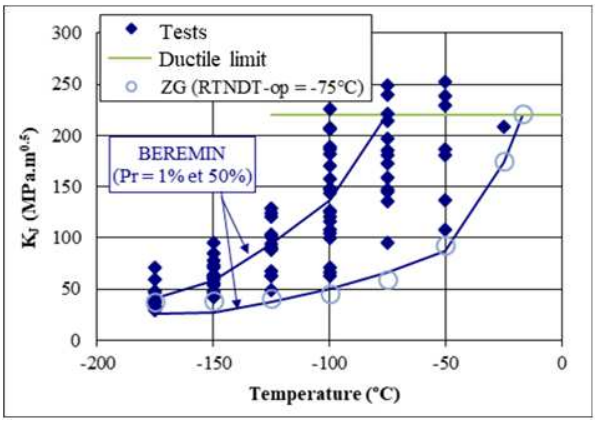

Figure 1: Toughness data for the low alloy 16MND5 steel [4]

For this material, a RT_{NDT} value was optimized based on the tests (noted $RT_{NDT\text{-}op}$) in order to envelop the data with the codified toughness curve ($RT_{NDT\text{-}op}$ = -75°C). On the fig. 1, the solid blue symbols represent the test data while the blue lines correspond to the 1% and 50% failure probability predicted by the BEREMIN model.

Additionally, it can be seen that the local model associated with a 1% probability of failure is in very good agreement with the codified RCC-M curve readjusted with $RT_{NDT\text{-}op}$ (represented here by the open circles).

Data for the C-Mn material:

Only few data are available regarding the description of the brittle to ductile transition for the C-Mn steel (material constituting the secondary loop and some auxiliary piping of PWRs). Some data were produced

by CEA with a series of tests carried out for the base metal P265GH, at low temperature, as part of internal R&D action dedicated to brittle fracture. Although much less data than the FISTER campaign are available, these data have the advantage of covering the transition of the material. They are thus used here for calibrating the BEREMIN model.
Within this program, toughness tests were carried out on notched CT20 specimens (CT20 reduced to 15mm and with 20% lateral notches). Based on the available data, the T_0 fit gives: T_0 = -145°C. The reference equivalent temperature as defined in [1] for defining the envelope toughness curve of the material is thus: $RT_{NDT\text{-}eq} = T_0 + 40°C = -105°C$

Like previous campaign, the BEREMIN model is calibrated through FEM. However, doing this calibration, it was rapidly shown that CT specimen were encountering generalised plasticity at fracture, especially at the highest temperature. Given the very large size of the plastic zone, it does not seem reasonable to integrate the probability of failure over the entire plastic zone as is done in the 2 parameters BEREMIN model. We then preferred here a 3-parameter model integrating a threshold stress. The latter, determined on Notched Tensile specimens at very low temperature as prescribed in [5], was fixed at σ_{th} = 1350 MPa, representing an average value between the available data for the family of material.

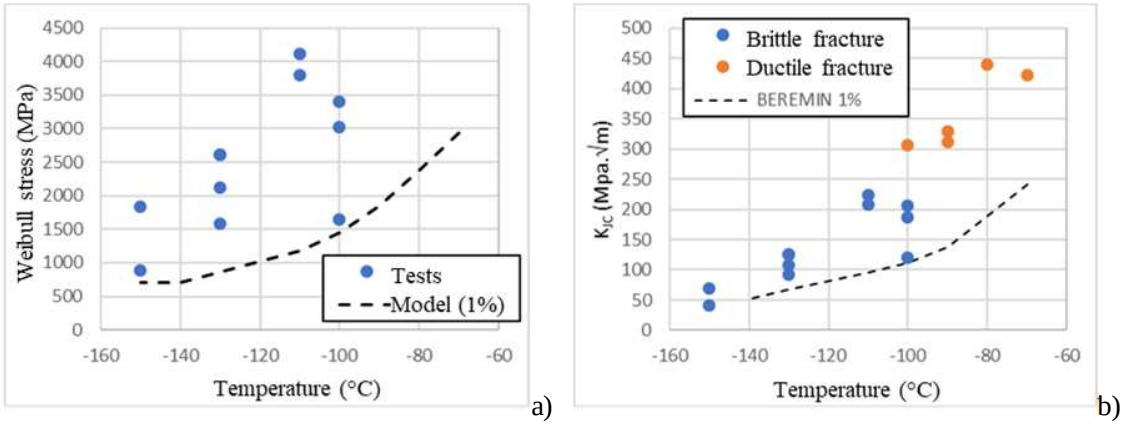

a) b)

Fig. 2: Data for the C-Mn steel, a) critical Weibull stress, b) minimum toughness curve

Given this threshold value, the module m (fixed at m = 4) and a $\sigma_u(T)$ evolution were fitted in order to define a critical Weibull stress (σ_W) corresponding to 1% probability of failure was defined (see fig. 2a). This critical Weibull stress provides a reasonable envelop of the toughness data within the interval -140°C to -70°C (fig. 2a and 2b).

INDUSTRIAL CONFIGURATIONS

Large cylindrical vessel containing a longitudinal inner crack

Model and loading description:

The industrial configuration investigated for the low alloy steel material is the one of a cylindrical shell containing an inner longitudinal surface defect and submitted to a pressurized thermal shock. This vessel is defined by its internal radius (2142 mm) and its thickness (114 mm). The surface defect is assumed to be a long one so that a 2D model could be used.
Regarding the WRS, these are postulated and introduced in the model through an initial radial and circumferential strain gradient. This strain gradient is self-balancing through the thickness (fig. 3).
Within the modelling, the maximum of the opening stress at the inner skin (denoted RS in the following graphs) is parametric and varies from 0 to 300 MPa. The other variable parameters in the modelling are the initial temperature of the cold thermal shock (noted T_{ini}), the temperature variation (six different thermal shocks are considered, numbered from 1 to 6), and the crack size (a = 5, 10 or 20 mm).

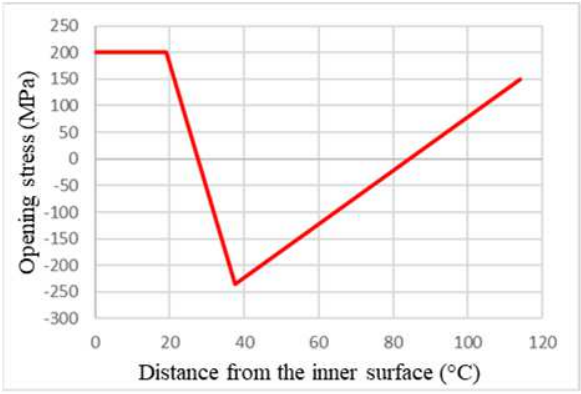

Figure 3: Stress distribution through the thickness for the vessel (here for RS = 200 MPa)

The different loading conditions adopted in the parametric FEM are given in table I. One should note that the selected temperatures have no physical meaning. They are defined as functions of $RT_{NDT\text{-}op}$ in order to be representative of loading configurations encountered in industrial applications.
It should be noted that, for some transients, the initial temperature T_{inpi} is defined according to the size of the defect so that the maximum of K_J is reached at the same temperature for the 3 defect sizes (this is the case for transients 3 to 6). For each modelling configuration, two calculations are carried out, one without WRS, the other with WRS. Those modelling are providing the energy release rate G (including or not the RS contribution) and the Weibull stress σ_W. K_J is then derived from G through the relation:

$$K_J = \sqrt{\frac{E.G}{1-\nu^2}}$$

In all cases, the stress-strain curves are depending on the temperature, those curves being provided in [4].

Results analysis

The fig. 4 is representing an example of K_J evolution (for global approach) and σ_W (for local approach) as a function of temperature (evolutions for the transient 5 corresponding to modelling #13 to #15 in table I).

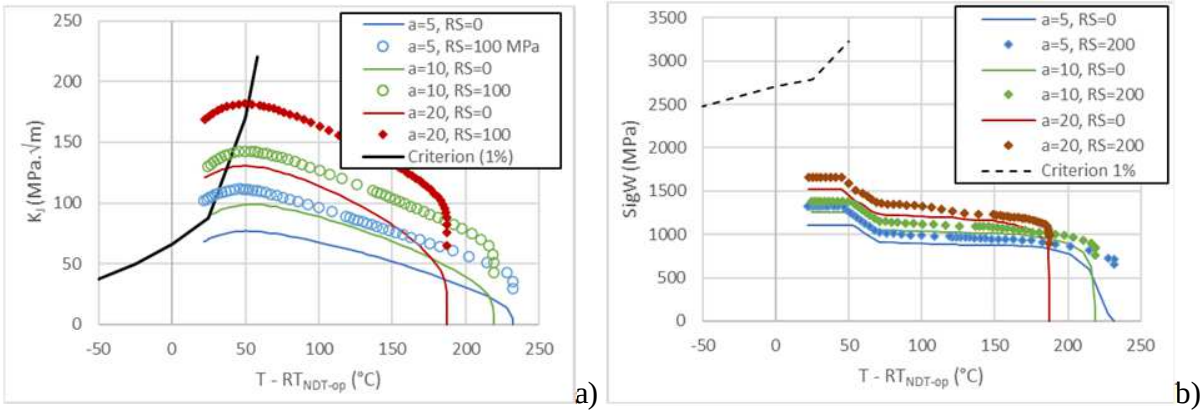

a) b)

Figure 4: Example of fracture mechanics parameters evolution during the thermal shock

The main observation form those graphs are the following:

- For the chosen transient, one finds the classic evolution of the K_J parameter during a cold thermal shock, with an increase in the first phase of loading, a maximum, then a decrease.

- For the Weibull stress σ_W, when the initial temperature of the transient is relatively high as this is the case in this example, it remains at very low levels. The evolution increases then stabilize since the model considers the active plasticity.
- One can observe that the addition of WRS leads to a very significant increase in the global approach parameter K_J, and much lower with regard to the local parameter σ_W.
- The comparison of the two types of criterion illustrates the significant conservatism of the global criterion with, in the #15 transient configuration (a = 20mm with WRS), a global approach criterion which predicts fracture (considering Warm Pre-Stressing effect – WPS) while the local approach predicts a significant margin: the ratio between the threshold curve and σ_W of the order of 2.

Based these representations for all the investigated transients, a quantification of the impact of WRS on the loading parameters and on the margins is proposed (considering WPS effect). For this, the following synthetic representations are proposed:

- We determine for each loading condition and the loading parameter (K_J or σ_W) at the maximum of K_J. This max of K_J is not depending on WRS and is representative of the fracture risk under cold thermal shock (according to the WPS principle).
- For this maximum, we define the ratios between calculated loading parameters with and without WRS. This representation makes it possible to quantify the amplification of the loading parameter due to the presence of WRS.

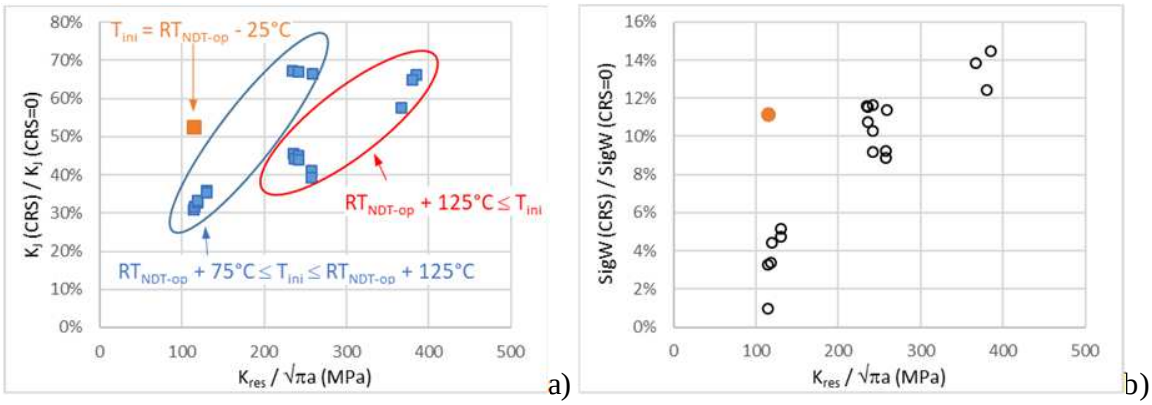

Figure 5: Quantification of the influence of the WRS on the loading parameters

These two ratios are shown in Fig. 5 as a function of the normalised Stress Intensity Factor (SIF) $K_{res}/\sqrt{(\pi.a)}$ (K_{res} being the SIF associated to the WRS distribution):

- On the left graph corresponding to global approach, we note a very severe amplification of the loading parameter. This amplification is relatively dispersed and varies from +30% to +70%. The orange point, corresponding to the configuration #0 (thermal shock with a low T_{ini}), is rather at the left of the dispersion without really detaching from it.
- On this same graph, T_{ini} is obviously an important parameter with respect to this amplification since the points can be grouped by intervals of initial temperatures.
- On the right graph, we see that the amplification corresponding to the local approach parameter is much lower: it peaks at 15%.
- The point corresponding to transient #0 is clearly distinguished, but the other points are all relatively well grouped together. Thus, provided that T_{ini} is high enough (the transient starts outside the ductile to brittle transition), the parameter $K_{res}/\sqrt{(\pi.a)}$ constitutes the dominant parameter, which is no longer the case for T_{ini}.

To clearly highlight the excessive conservatism of the global approach in comparison to the local approach, we represent in fig. 6a one ratio as a function of the other. As it can be seen on this representation, the global approach is much more severe than the local approach. The amplification associated with the first criterion is at least 3 times greater than that of the second. Note that, in this representation, the orange point (transient #0) has joined the other points.

We can also directly compare the margins between the two kinds of criterion. On fig. 6b, the margin determined through the global approach criterion without WRS is compared with the margin determined through the local approach criterion with WRS. As it can be seen in this graph, the first margin is larger or equal to the second, even for the orange point where the behaviour is quasi-elastic. On can conclude that the intrinsic conservatism of the global approach therefore envelops the moderate supplement provided by the presence of WRS, independently of the transient, the size of the defect or the level of WRS.
One explanation regarding this observation should be that, for a variable temperature loading, the global approach criterion does not consider the stress history, and in particular the evolution of the yield stress with temperature. This evolution is implicitly considered within the local approach criterion since it relies directly on the calculated local stresses.

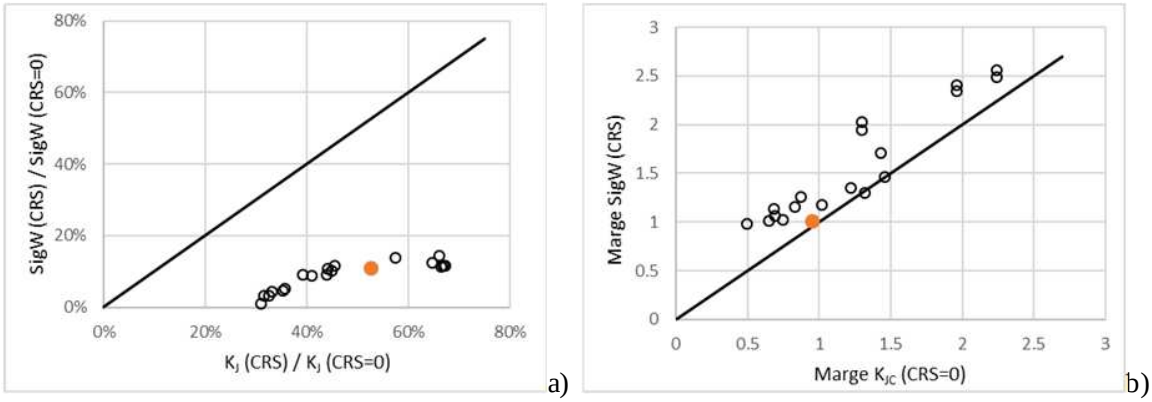

Figure 6: a) Amplification of the loading parameters b) Comparison of margins

Pipe submitted to a bending load

Model and loading description:

The investigated geometrical configuration for the C-Mn pipe is defined by an inner radius (343.3 mm) and a thickness (38.7 mm). An outer surface defect is assumed. This defect has a semi-elliptical shape defined by its depth (a = 10 mm) and elongation ratio (c/a = 3, c being the half-length on surface).
The loading imposed to this pipe is a global bending, representative of a seism loading at cold temperature. The constitutive laws used here are those of the base metal P265GH used for the calibration of the 3 parameters BEREMIN model.

Three temperatures in the brittle-ductile transition of the material are selected for modelling: -100°C (corresponding to RT_{NDT-eq} + 5°C), -85°C (RT_{NDT-eq} + 20°C) and -70°C (35°C RT_{NDT-eq} + 35°C, temperature where initiation is only ductile on CT specimens).
The WRS field is postulated and opens the external surface defect (Fig. 7). Several levels of this WRS distribution are investigated from 100 MPa to 400 MPa. Again, the mean level imposed to the crack surface is noted RS.

In accordance with the BEREMIN model needs and in consistency with the calibration on CT specimens, a mesh with square elements of 50µm² perpendicular to the crack front was developed. The model is composed of quadratic elements. It contains approximately 100000 nodes, which remains reasonable for this type of modelling. The following loading parameters are determined with this surface defect model:

- The elastic-plastic SIF K_J at the deepest point of the crack: this is the relevant value with respect to the risk of fracture according to the global approach because, for the kind of elongated defect like the one studied here, it is the most loaded point.
- The Weibull stress σ_W which is representative of the stress all along the crack front since it corresponds to the integration of the main stresses within the plastic volume around the crack tip.

Two parameters are varying in the parametric FEM: the temperature and the level or WRS. Table II gives an overview of the investigated configurations.

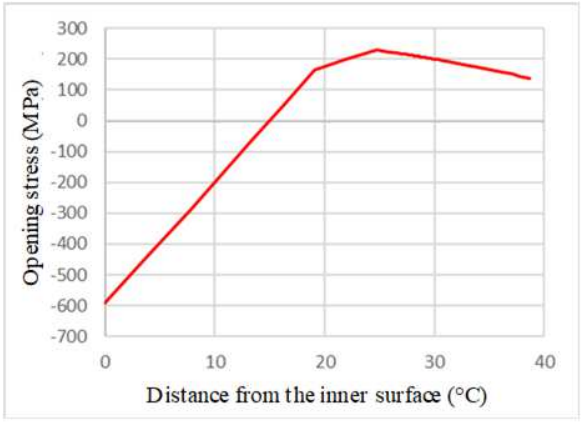

Figure 7: Assumed WRS distribution for the C-Mn pipe (for RS = 200 MPa)

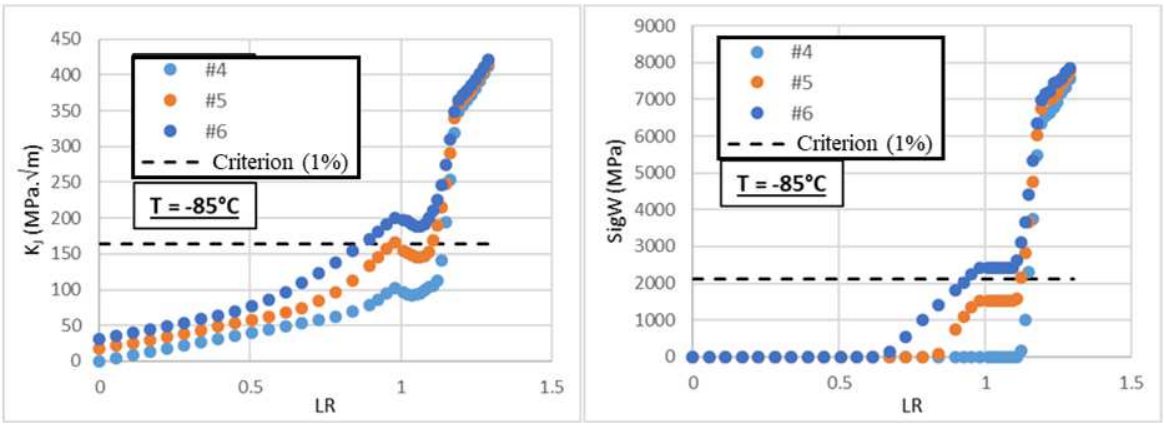

Figure 8: Evolution of the loading parameters, K_J (on left), Weibull stress σ_W (on right)
(#4 to #5 are corresponding to the modelling condition given in table II)

Results analysis

The fig. 8 gives an example of the evolution of the loading parameters K_J and σ_W for the intermediate temperatures. On this figure, the chosen parameter for defining the level of loading is L_R characterizing the level of plasticity in the pipe. L_R defined here considers the presence of the defect and is defined by:

$$L_R = \lambda . \frac{M}{4 . r_m^2 . t},$$

Where M is the bending moment imposed to the pipe, r_m the mean radius, t the thickness and λ the geometric parameter which considers the presence of the defect. The latter calibrated numerically and is $\lambda = 1.12$.
On the Fig. 8, the thresholds (the dotted lines) are corresponding to the values determined at the chosen loading temperatures on fig. 2 (K_{JC} and σ_W for 1% probability of failure).

The observations that can be made on the evolutions of fig. 8 are as follows:

- The evolutions of the parameters K_J and σ_W are different: the parameter K_J increases from the beginning of the loading while σ_W remains null then increases brutally. For this last parameter, this type of evolution is to be associated to the 3 parameters BEREMIN model, and in particular to the threshold stress σ_{th} = 1350 MPa.
- All the curves are presenting an inflection or a plateau for $L_R \sim 1$. This value corresponds to the transition from confined plasticity to generalized plasticity, it therefore corresponds to a sudden increase in the size of the plastic zone associated with the long Lüders' plateau of this material. This plateau is a particularity of the C-Mn steel which has some consequences on the crack tip loading and the interaction between the external loading and the WRS (see [6]).
- After this level, for $L_R \sim 1.15$, the curves meet before going up, both for the global approach and for the local approach: we can consider that this corresponds to the end of plateau and that the pipe undergoes generalised plasticity and thus all the WRS have been erased by plasticity.
- We see through those figures that, for this geometry and this type of loading, the presence of WRS increases the two loading parameters. Contrary to the case of the thermal shock, the evolutions observed are similar between the global approach and the local approach.

To represent this last result, we define the critical value of L_R (denoted L_{RC}) for which the critical values (dotted lines on fig. 8) are exceeded. We then plot in Fig. 9a the reduction of this L_{RC} for local approach as a function of its equivalence for global approach. This figure merges all the modelling configurations.
We show through this figure that the global approach remains more severe than the local approach, but the difference is less pronounced than for the previous thermal shock configuration.

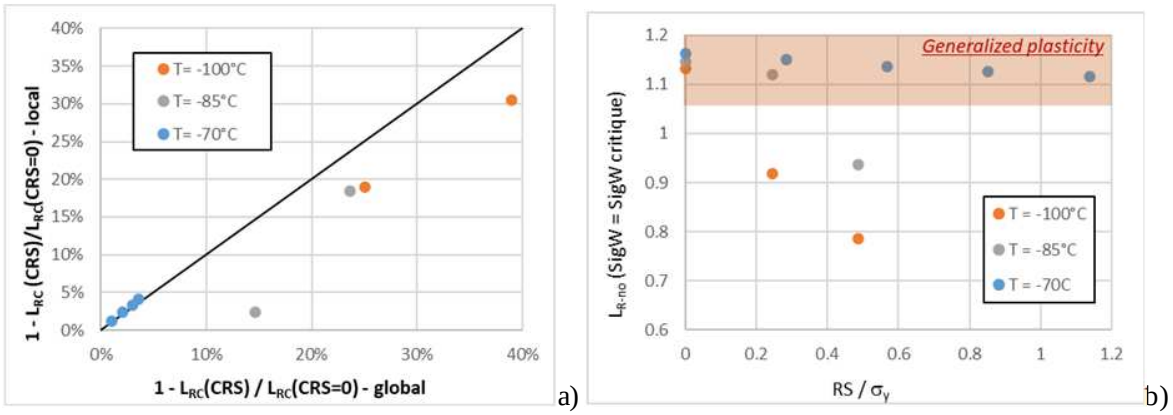

Figure 9: a) Comparison of the critical LR reduction due to the presence of WRS
b) Critical L_{RC} as a function of the WRS level

If we focus on local approach, another way to present the numerical result is to plot the critical L_{RC} as a function of the WRS level (fig. 9b). The parameter represented here is $L_{R\text{-}no}$, that is the nominal L_R parameter defined without considering the presence of the defect ($\lambda = 1$ in the L_R definition).
This graph highlights two domains: the domain where crack initiation is reached before generalized plasticity and the domain where generalized plasticity is reached at first. In the first case, there is an effect of the WRS, otherwise not no effect is observed since the WRS are removed by the generalised plasticity.

Base on those results, we can conclude that two parameters are governing the influence of the WRS on fracture for this configuration of piping subjected to a mechanical loading: the level of WRS and the material yield stress governing the limit load of the pipe.

DISCUSSION – THRESHOLDS PROPOSITION

For low-alloy steel subjected to thermal shock, the global approach turns out to be excessively conservative. The points that can be put forward to explain this observation are the following:

- To be sufficiently severe, the thermal shock must necessarily have an initial temperature in the ductile domain of the material. At this temperature, the stresses which appear at the beginning of the transient are attenuated by the low level of the yield stress. For this type of loading and material, the history of plasticity at the crack tip is significant: The thermal shock loading being imposed strains, a large part of the '*fracture engine*' is dissipated at hot temperature at the beginning of the thermal loading.
- The thermal shock loading is of the same nature as the WRS, namely imposed strains. This is thus the complete loading which is affected by plasticity, and not only the WRS.

For this type of loading and material, regarding the definition of a threshold and based on our numerical results, we can look at the problem at two levels:

- If we look at the impact of WRS on the local approach criterion, this remains moderate (less than 15%) and vanishes for the lowest levels of WRS (see fig. 6a). In practice, the modelling is showing that for a parameter μ below 25%, the impact of WRS is no longer observed. μ is here an averaged and normalised SIF associated to the WRS distribution defined as:

$$\mu = \frac{K_{res}}{\sigma_y . \sqrt{\pi . a}},$$

- The impact being moderate in all cases, it is covered by the intrinsic conservatism of the global approach which considers the failure criterion isothermally (see fig. 6b).

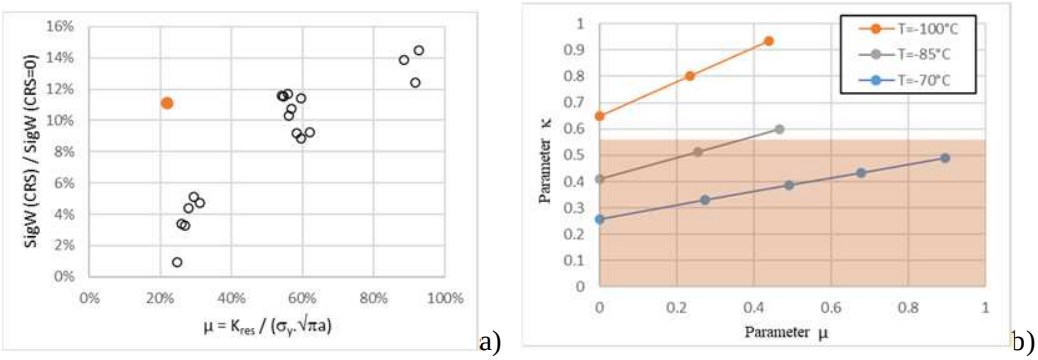

Figure 10: Impact of WRS, a) Low alloy steel configuration, b) C-Mn configuration

We can therefore conclude that the WRS are not to be taken into account for the weld configurations encountering a Post Weld Heat Treatment (PWHT) ensuring a WRS level μ < 25%%, as for example PWHT in a furnace.

For welds where one cannot consider a level μ < 25% (see fig. 10a), the present study shows that in our modelling configuration the WRS could be ignored within the framework of the conventional global approach if the initial temperature of the transient is higher than RT_{NDT} + 75°C (corresponding to the domain covered by this study). The intrinsic conservatism of the global approach covers the impact of WRS on the fracture risk. One important point to notice is that we are not talking here about a peak of WRS, but of stresses distributions normalised through the SIF (μ parameter) which appears to be the relevant parameter. Those results are of course to be confirmed by further developments.

For C-Mn steel, the study carried out here shows that it is possible to define a 3 parameters local approach model for this family of material. The specificity here is that it is necessary to introduce a stress threshold stress σ_{th} so as not to integrate the Weibull stress within a rapidly extending plastic zone.

With respect to the influence of WRS, and compared to thermal shock, the modelling carried out here shows that the observed behaviour is significantly different. The mechanical loading at constant temperature and the long Lüders plateau on tensile curve observed for this family of material are influencing the results: the effect of WRS determined via the local approach criterion is relatively significant, when it exists, and of the same order of magnitude as that determined via the global approach criterion.
We can then conclude that for this pipe configuration, two parameters are governing the influence of the WRS: their level and the level of the yield stress (through the pipe limit load). In other words: either the crack initiation can be reached in the quasi-elastic domain and there is a significant effect, or it is not the case and there is no longer any effect.

Being a competition between plastic collapse and brittle fracture, a possibility to separate the two previous situations is to rely on the parameter κ proposed in [7] to define a limit. This parameter corresponds to the ratio of the R6 diagram parameters K_r / L_R, a low value meaning that it is the plasticity which dominates, while a high value meaning that it is the fracture which dominates.
Since we are interested in the initiation in the presence of WRS, if we add their contribution to a primary membrane stress, the slope κ takes the following form:

$$\kappa = \frac{\sigma_y.(1+\mu).\sqrt{\pi.a}}{K_{JC}},$$

As illustrated in fig. 10b, this parameter is a good candidate for defining some limit. In this figure, the orange area is corresponding to the orange area of the figure 9b where the WRS can be neglected.

CONCLUSIONS AND PERSPECTIVES

This note presents the numerical modelling carried out in support of the development of criteria or thresholds for the definition of the domain where the WRS are important, or on the contrary they are not, with respect to the risk of brittle failure. To do this, two configurations are investigated:

- A large low-alloy ferritic steel vessel subjected to thermal shock loads.
- A C-Mn steel pipes subjected to a global bending moment representative seism situation at cold temperature.

Based on the obtained numerical results, the following recommendations are initiated:

- For thick components encountering a PWHT ensuring a WRS level $\mu < 25\%$ (as for example PWHT in a furnace) and subjected to a cold thermal shock, WRS can be neglected in all cases.
  For welds where $\mu > 25\%$, it appears that the intrinsic conservatism of the conventional global approach covers the impact of WRS if the initial temperature of the transient is higher at RT_{NDT} + 75°C (the limit of the domain covers by the present modelling). This observation has to be confirmed in further work.
- For ferritic steel pipes subjected to mechanical loading, a parameter κ and an associated threshold appears to be good candidates for defining limits: for the investigated configurations, if $\kappa < 0.55$, the WRS appears to be negligible with respect to the risk of brittle fracture because generalized plasticity appears before reaching the crack initiation criterion.
  On the contrary, if $\kappa > 0.55$, WRS are to be considered in the analysis. The global approach appears to be suitable because it only moderately overestimates the impact of WRS.

The outline of the thresholds having been initiates, additional developments can be envisaged to consolidate and/or clarify them. These developments are both numerical and experimental.
On the numerical side, the developments should mainly concern piping, with the analysis of different geometric or loadings: thinner tubes and/or more complex geometries (elbows for example) to test the relevance of the κ parameter proposed to quantify the scale effect. Cold thermal shock situations combined with mechanical loading should also be investigated.
Additionally, even if it is not very pronounced for ferritic material, the effect of the mismatch between the base metal and the weld metal could also be investigated because it is a potentially significant source of

conservatism for welded joints. Regarding the parameter κ, the question concerns the yield stress to be considered in the parameter μ: the one of the base metal or the weld metal?

On the experimental side, as it has been shown in the literature survey [1], the challenge is more difficult because the implementation of known and reliable WRS, without altering the material is a difficult exercise. This path is however important for confirming the relevance of the local approach criterion in the presence of WRS, both for low alloy steel and for C-Mn steel. This local approach criterion validation is essential to be able to transpose results from specimen to real components.

ACKNOWLEDGMENT
The authors would like to warmly acknowledge their colleague Déborah Clément from CEA for sharing her test data (and fruitful discussion) on the P265GH C-Mn steel. Without those data, this prospective numerical work on pipes couldn't have been done.

REFERENCES
[1] S. Chapuliot *et al.*, Consideration of welding residual stresses within the fracture mechanics assessment of nuclear components – Part 1: Bibliography analysis, SMiRT-26, Berlin/Potsdam, Germany, (2022)
[2] R.G. Hurlston , J.K. Sharples, A.H. Sherry, Understanding and accounting for the effects of residual stresses on cleavage fracture toughness measurements in the transition temperature regime, International Journal of Pressure Vessels and Piping 128 (2015) 69-83
[3] BEREMIN, FM. A local criterion for cleavage fracture of a nuclear pressure vessel steel. Metall Trans A 1983;14A:2277–87
[4] S. Chapuliot *et al.*, Thermomechanical analysis of thermal shock fracture in the brittle/ductile transition zone. Part I: description of tests, Engineering Fracture Mechanics 72 (2005) 661–673
[5] V. Le Corre *et al.*, Transferability of cleavage appearance temperature from laboratory specimen to structure, EUROMECH-MECAMAT meeting, 9th European Mechanics of Materials Conference, Moret sur Loing (2006)
[6] S. Chapuliot *et al.*, Status of the on-going R&D dedicated to the residual stresses consideration in Fracture Mechanics Assessment, SMiRT-24, BEXCO, Busan, Korea (2017)
[7] S. Chapuliot, Consideration of residual stresses in Fracture Mechanics Assessments, ATLAS+ REPORT D2.7-WP2

Table I: FEM configurations for the Vessel configuration

Transients	**FEM number**	**T_{ini}: Initial Temperature**	**DT: Temperature variation**	**RS**	**Defect depth**	**$T_{ini} - RT_{NDT-op}$**
(0)	#0	-100°C	-90°C	100 MPa	5 mm	-25°C
(1)	#1	0°C	-180°C	100 MPa	5 mm	75°C
	#2	0°C	-180°C	100 MPa	10 mm	75°C
	#3	0°C	-180°C	100 MPa	20 mm	75°C
(2)	#4	50°C	-180°C	100 MPa	5 mm	125°C
	#5	50°C	-180°C	100 MPa	10 mm	125°C
	#6	50°C	-180°C	100 MPa	20 mm	125°C
(3)	#7	107°C	-280°C	200 MPa	5 mm	182°C
	#8	94°C	-280°C	200 MPa	10 mm	169°C
	#9	62°C	-280°C	200 MPa	20 mm	137°C
(4)	#10	42°C	-180°C	200 MPa	5 mm	117°C
	#11	34°C	-180°C	200 MPa	10 mm	109°C
	#12	13°C	-180°C	200 MPa	20 mm	88°C
(5)	#13	157°C	-280°C	200 MPa	5 mm	232°C
	#14	144°C	-280°C	200 MPa	10 mm	219°C
	#15	112°C	-280°C	200 MPa	20 mm	187°C
(6)	#16	157°C	-280°C	300 MPa	5 mm	232°C
	#17	144°C	-280°C	300 MPa	10 mm	219°C
	#18	112°C	-280°C	300 MPa	20 mm	187°C

Table II: FEM configurations for the C-Mn pipe

Calculs	**Température**	**Niveau RS**	**RS/σ_y**
#1	-100°C	0	0
#2	-100°C	100 MPa	0.24
#3	-100°C	200 MPa	0.49
#4	-85°C	0	0
#5	-85°C	100 MPa	0.26
#6	-85°C	200 MPa	0.53
#7	-70°C	0	0
#8	-70°C	100 MPa	0.28
#9	-70°C	200 MPa	0.57
#10	-70°C	300 MPa	0.85
#11	-70°C	400 MPa	1.14